Chemosphere 76 (2009) 1075–1081

Contents lists available at ScienceDirect

Chemosphere

journal homepage: www.elsevier.com/locate/chemosphere

Environmental aging of polycyclic aromatic hydrocarbons on soot and its effect on source identification

Daekyun Kim [a,1], Benjamin M. Kumfer [b], Cort Anastasio [a,c], Ian M. Kennedy [b], Thomas M. Young [a,d,*]

[a] Agricultural and Environmental Chemistry Graduate Group, University of California, One Shields Avenue, Davis, CA 95616, USA
[b] Department of Mechanical and Aeronautical Engineering, University of California, One Shields Avenue, Davis, CA 95616, USA
[c] Department of Land, Air, and Water Resources, University of California, One Shields Avenue, Davis, CA 95616, USA
[d] Department of Civil and Environmental Engineering, University of California, One Shields Avenue, Davis, CA 95616, USA

ARTICLE INFO

Article history:
Received 9 January 2009
Received in revised form 12 April 2009
Accepted 14 April 2009
Available online 13 May 2009

Keywords:
PAH
Soot
Environmental aging
Two-phase degradation
Source apportionment

ABSTRACT

Soot-associated PAHs were exposed to simulated sunlight to investigate disappearance rates under environmental aging conditions and to examine the robustness of diagnostic ratios for PAH source apportionment. Naphthalene, acenaphthylene, acenaphthene, and fluorene showed an obvious two-phase disappearance in all experiments while phenanthrene and anthracene exhibited this behavior for all but the highest soot loading. The first phase loss is 5–40 times faster than the second phase loss and occurred within 3 h for naphthalene, acenaphthylene, acenaphthene, and fluorene and within 10 h for phenanthrene and anthracene. Two-phase disappearance was not observed for any of the higher molecular weight PAHs with 4–6 rings. Each PAH has a unique loss rate via photodegradation and volatilization and these rates of some PAHs were affected by soot loadings; phenanthrene and anthracene showed similar rates in the first phase and increased loss rates in the second phase as soot loading increased. In the absence of light, the loss of PAHs was related to both temperature and molecular characteristics. Due to differences in disappearance rates of individual PAHs under illumination over extended times, prolonged exposure to sunlight could change the interpretation of some diagnostic ratios used previously for PAH source identification. This result indicates that more consistent and accurate methods that take into consideration the longevity of particulate PAHs are needed for reliable source apportionment.

1. Introduction

Since polycyclic aromatic hydrocarbons (PAHs) are ubiquitous, and some PAHs are carcinogenic and/or mutagenic, their fate and transport in the environment has been extensively investigated (Jacob, 1996; Hannigan et al., 1998; Douben, 2003). Many attempts have been made to determine the primary sources of PAHs observed in air, water, sediment, and soil samples by using selected marker compounds and homologue distribution patterns as well as specific PAH ratios. For example, to distinguish PAHs of petrogenic origin (i.e., PAHs derived from liquid petroleum before combustion) from those of pyrogenic origin (i.e., PAHs derived from combustion processes), the ratios of anthracene to phenanthrene and fluoranthene to pyrene have been widely used (Sicre et al., 1987; Yunker et al., 2002). The ratios of the sum of low molecular weight (2–3 rings) PAHs to the total PAHs, and the sum of major combustion-specific compounds (fluoranthene, pyrene, benzo[*a*]anthracene, chrysene, benzo[*b*]fluoranthene, benzo[*k*]fluoranthene, benzo[*e*]pyrene, benzo[*a*]pyrene, indeno[*1,2,3-cd*]pyrene) to the total, have also been used as diagnostic indicators to infer possible PAH sources (Prahl and Carpenter, 1983; Boehm and Farrington, 1984; Hwang and Foster, 2006). It has also been documented that the ratios of alkylated phenanthrenes to phenanthrene, benzo[*b*]fluoranthene to benzo[*k*]fluoranthene, and benz[*a*]anthracene to chrysene indicate the relative contributions of PAHs from wood combustion, coal burning, and vehicle operation, respectively (Berner et al., 1995; Dickhut et al., 2000). These selected ratios have been applied to identify major sources of PAHs in field samples collected from the atmosphere, surface waters, sediments, soils, and even vegetation and bivalves (Prahl and Carpenter, 1983; Boehm and Farrington, 1984; Sicre et al., 1987; Berner et al., 1995; Dickhut et al., 2000; Yunker et al., 2002; Dreyer et al., 2005; Oros and Ross, 2005; Hwang and Foster, 2006; Orecchio, 2007). Since PAHs in environmental samples have multiple origins rather than a single one – and since some PAH ratios in a certain sample sometimes contradict others – it is not always simple to predict the major PAH sources and their relative contributions. PAHs have been reported to display differential degradation rates during transport and deposition (Schauer et al., 1996; Zhang et al., 2005). Differences in volatility, phototransformation

* Corresponding author. Address: Department of Civil and Environmental Engineering, University of California, One Shields Avenue, Davis, CA 95616, USA. Tel.: +1 530 7549399; fax: +1 530 7527872.
E-mail address: tyoung@ucdavis.edu (T.M. Young).
[1] Present address: School of Public and Environmental Affairs, Indiana University, Bloomington, IN 47405, USA.

0045-6535/$ - see front matter © 2009 Elsevier Ltd. All rights reserved.
doi:10.1016/j.chemosphere.2009.04.031

rates, and bio-degradation rates of individual PAHs could lead to changes in PAH profiles in samples aged prior to collection; in such cases, source apportionment by conventional methods would be much more complicated.

While PAHs are produced from various combustion sources, soot is also generated from volatiles formed within flames that subsequently produce carbon-rich material through a complex mass growth process (Schmidt and Noack, 2000). Pyrogenic PAHs are suggested to be partially occluded in the soot matrix during the incomplete combustion process, to be trapped in micropores, or to have extremely high affinities for the aromatic flat surfaces of soot (Readman et al., 1984; Eganhouse, 1997). Phototransformation of particulate PAHs is known to be one of the most important degradation processes (Kamens et al., 1988). The photolytic behavior of PAHs in particulate matter is dependent on the chemical and physical properties of substrates such as color, size, carbon content, surface area, and particle porosity. Carbonaceous materials such as fly ash, carbon black, and soot have been reported to protect sorbed PAHs from degradation in the atmosphere, water column, and sediments, while PAHs on the surfaces of silica gel and alumina decayed quickly (Korfmacher et al., 1980; Behymer and Hites, 1985, 1988). However, determination of the intrinsic photodegradation rate constants of PAHs in soot particles considering the layer thickness and the aging effect on the source apportionment of PAHs has not been studied. This study focuses on quantifying the loss rates of soot-associated PAHs under controlled laboratory conditions of temperature and irradiation. A major objective is to determine the extent to which differences in such loss processes among PAHs might affect commonly used indicators of PAH sources.

2. Experimental

2.1. Soot generation

Soot particles were obtained from a rich premixed ethylene flame stabilized on a standard laboratory circular flat burner (McKenna Products, Inc., Pittsburg, CA). A mixture of ethylene and filtered air with an equivalence ratio of 1.73 (C/O = 0.58) was delivered to the burner at a total flow rate of 9.7 L min^{-1}. Heat transfer to the burner was maintained using a 0.5 L min^{-1} flow of cooling water. The flame was surrounded by a shroud of nitrogen gas to minimize the diffusion of oxygen into the flame from the ambient air. Soot particles were collected using a dilution probe positioned at a height of 20 mm from the burner surface. Nitrogen gas was introduced into the dilution probe to quench chemical reactions. Details regarding the probe construction can be found elsewhere (Yu et al., 1998). The post-flame gas was stabilized using a stainless steel screen attached to the sampling probe. The particles were deposited onto 47 mm diameter PTFE membrane filters (Sartorius Biotech Inc., Edgewood, NY) with a pore size of 0.2 μm. The determination of organic carbon (OC) and elemental carbon (EC) was obtained by the thermal–optical transmission technique using a carbon aerosol analysis instrument (Sunset Laboratory Inc., Forest Grove, OR). A temperature profile based on the NIOSH 5040 protocol was used (NIOSH, 1999).

2.2. Irradiation of soot-associated PAHs

To mimic environmental aging conditions with exposure to sunlight, soot particles were irradiated for 24 h at ambient temperature with the output from a high pressure 1000 W xenon arc lamp (Osram Sylvania Inc., XBO 1000 W/HS OFR) after it was passed through a dichroic cold mirror in the lamp housing (to only transmit wavelengths between 300 and 500 nm). PAH concentrations were determined as the amount of PAHs per unit mass of soot by weighing pieces of soot-containing PTFE filters before and after illumination. To obtain first order decay rate constants of PAHs on soot, each filter was cut into eight sectors. The sectors of a filter were placed on a Teflon plate, illuminated for a given time, and taken out for analysis. A homogeneity test was performed to ensure that soot particles were evenly spread on the filters; the deviation between sectors was less than 6% of the average PAH concentrations. Photon flux values in each experiment were monitored by measuring the rate constant for loss of aqueous 2-nitrobenzaldehyde (2NB) as a chemical actinometer.

2.3. Dark controls

During illumination the temperature of the filter increased gradually until it stabilized at 36 °C. Hence, to investigate possible contributions of volatilization or other thermal degradation processes to the disappearance of PAHs, soot containing PTFE membrane filters were divided, placed on watch glasses, wrapped with aluminum foil, and located in an environmental chamber maintained at 36 °C for 24 h (2.1 and 12.7 mg/filter soot samples) or 18 °C for 48 h (4.9 mg/filter soot sample).

2.4. Extraction, clean-up and analysis

After illumination, sectors cut from PTFE filters with soot-associated PAHs were separately introduced into a Soxhlet extractor, spiked with deuterated surrogates (naphthalene-d_8, acenaphthene-d_{10}, phenanthrene-d_{10}, and chrysene-d_{12}), and extracted with dichloromethane for 12 h. All extracts were concentrated using a rotary vacuum evaporator (Buchii Rotavapor R-3000) to 3–5 mL, and subsequently cleaned up and fractionated by column chromatography using 40 g of alumina (80–120 mesh) activated at 450 °C for 4 h and deactivated (4%) with water before use. The column was eluted with 120 mL of 1:1 (v/v) pentane/dichloromethane mixture to remove retained compounds. Final volume of the extracts was 0.5–1 mL after rotary vacuum evaporation and nitrogen blow-down. Prior to instrumental analysis, a deuterated standard (pyrene-d_{10}) was added to check analytical efficiency.

Identification and quantification of 16 PAHs – naphthalene (Naph), acenaphthylene (Acy), acenaphthene (Ace), fluorene (Flu), phenanthrene (Phe), anthracene (Ant), fluoranthene (Flt), pyrene (Pyr), benz[*a*]anthracene (BaA), chrysene (Chry), benzo[*b*]fluoranthene (BbF), benzo[*k*]fluoranthene (BkF), benzo[*a*]pyrene (BaP), indeno[*1,2,3,-cd*]pyrene (InP), dibenz[*a,h*]anthracene (DaA), and benzo[*g,h,i*]perylene (BgP) – were accomplished using a Hewlett–Packard 6890 gas chromatograph equipped with a DB-5MS fused-silica capillary column (30 m × 1.25 mm ID, 0.25 μm film thickness) and a Hewlett–Packard 5973 mass selective detector. Helium was utilized as a carrier gas (1.3 mL min^{-1}). The oven temperature started initially at 60 °C, programmed for three temperature ramps, to 150 °C at 15 °C min^{-1}, to 220 °C at 5 °C min^{-1}, and to 310 °C at 10 °C min^{-1}, and held for 7 min. Injector and detector temperatures were 310 and 300 °C, respectively. The mass selective detector was operated in the electron ionization (70 eV) and the selected ion monitoring modes. Concentrations of individual compounds in the sample were calculated from the response factors determined using external standards. Calibration standards ranged from 62.5 to 2000 ng mL^{-1}. The method detection limit ranged from 0.09 to 0.76 ng mL^{-1}. A standard reference material (SRM2975, Diesel particulate matter) purchased from NIST (Gaithersburg, MD) was analyzed in the same manner as the soot samples. Measured PAH concentrations in the SRM were within 20% of certified concentrations.

3. Results and discussion

3.1. Soot characteristics and PAHs sorbed on the soot particles

The initial concentrations of soot-associated PAHs are given in Table 1, showing that Pyr, Flu, and BgP were the dominant species, contributing more than 50% to the sum of the 16 PAH concentrations. In contrast, DaA was not detected and Naph, Ace, and Chry were the least abundant PAHs on the soot particles. This PAH distribution pattern is similar to the typical PAH profile of diesel motor vehicle emissions (Lee et al., 2004). To investigate the effect of soot layer thickness on loss and phototransformation rates, soot samples were generated under identical conditions but different amounts were collected, yielding filters with 2.1, 4.9, and 12.7 mg of soot. PAH mass per soot mass was used as the concentration unit to calculate the kinetics of PAH disappearance.

The measured OC fractions of the samples used in this study were about 60%. Laboratory generated soot provides useful information for understanding combustion particles because it is produced under conditions that are reproducible and controllable.

3.2. Disappearance of PAHs during simulated sunlight illumination

The average first order rate constant for 2NB loss in the solar simulator ($0.016\ s^{-1}$) is approximately 20% higher than the measured value in Davis, California, USA, at solar noon on the summer solstice ($0.013\ s^{-1}$; Anastasio and McGregor, 2001). Thus, the 300–500 nm photon flux in the solar simulator is approximately the same as that for mid-latitudes during midday in summer.

Soot-associated PAHs can be categorized into three groups according to their loss rates under irradiation (Table 1). For the first group, the lowest molecular weight PAHs, an obvious two-phase loss was observed. Naph, Acy, Ace, and Flu were lost quickly over the first 3 h and then more slowly for the remainder of the experiment, independent of soot loading. The first phase loss rates are about 5–40 times higher than the second phase rates of these four PAHs. The rate constants obtained from the second phase loss of soot-associated Acy, Ace, and Flu are similar to each other and independent of soot loading. Soot loading masses did not depend systematically on either the first phase loss constants or normalized photon flux (j_{PAH}/j_{2NB}), suggesting that the variability may be random. For example, the highest first phase loss constants were observed on 4.9 mg/filter soot for Acy and Flu and on 12.7 mg/filter soot for Ace, respectively. Phe and Ant behave somewhat differently from the first four low molecular weight PAHs; the first loss phase lasted about 10 h on 2.1 and 4.9 mg/filter soot samples, whereas only a single loss mode was observed during 24 h of illumination on the 12.7 mg/filter soot sample. In the Phe and Ant cases, the first phase loss rates were 5–10 times faster than the second phase rates. The rate constants of these compounds in the second loss phase increased as the mass loading of soot increased, while the first phase rate constants of both compounds are very similar to one another, implying that both compounds have a similar loss mechanism and the thickness of substrates are not significant for their first loss phase. More than 80% of PAHs were lost in the first phase under illumination with a solar simulator. Flt and Pyr in 2.1 mg/filter soot might be categorized into the second group such as Phe and Ant. However, calculated first phase rate constants of Flt and Pyr were not significantly different from those for the single mode disappearance. In larger amount of soot, they showed an obvious single mode. The rest of the PAHs, those with 4–6 rings, however, did not exhibit the rapid initial loss and a single first-order rate characterized their disappearance over the 24 h experiment.

The aging process of particulate PAHs under sunlight includes both photochemical degradation and volatilization. Fig. 1 shows the disappearance rates of selected PAHs sorbed on soot particles under illumination and in the dark suggesting that photodegradation could be the main loss pathway of soot-associated PAHs deposited on land from the atmosphere rather than volatilization. Flu and Phe sorbed on 2.1 mg/filter soot had much higher rate

Table 1
Initial PAH concentrations on soot samples and first order loss constants during illumination and in the dark (h^{-1}).

	Initial conc.[a] (ng/mg soot)	2.1 mg soot						4.9 mg soot						12.7 mg soot					
		Illuminated (j_{2NB} = 0.016 s^{-1})[b]				Dark control (36 °C)		Illuminated (j_{2NB} = 0.020 s^{-1})[b]				Dark control (18 °C)		Illuminated (j_{2NB} = 0.013 S^{-1})[b]				Dark control (36 °C)	
		0–3.5 h	R^2	3.5–24 h	R^2	0–24 h	R^2	0–3 h	R^2	3–24 h	R^2	0–48 h	R^2	0–3 h	R^2	3–24 h	R^2	0–24 h	R^2
Naph[c]	87 (±17)	0.04	n/a[d]	0.004	0.49	0.005	0.37	0.21	n/a[d]	0.016	0.73	0.003	0.42	0.02	0.54	0.003	0.22	0.018	0.86
Acy	1300 (±400)	0.37	n/a[d]	0.026	0.92	0.054	0.98	0.80	n/a[d]	0.030	0.93	0.016	0.98	0.47	0.94	0.022	0.68	0.076	0.98
Ace	24 (±12)	0.37	n/a[d]	0.024	0.79	0.068	0.96	0.44	n/a[d]	0.033	0.50	0.018	0.97	0.54	0.99	0.014	0.16	0.073	0.97
Flu	180 (±37)	0.33	n/a[d]	0.025	0.89	0.035	0.97	0.54	n/a[d]	0.028	0.83	0.008	0.84	0.18	0.97	0.033	0.62	0.033	0.97
		0–9.6 h		9.6–24 h				0–8.9 h		8.9–24 h					0–24 h				
Phe	1600 (±410)	0.19	0.96	0.021	0.50	0.025	0.93	0.19	1.00	0.043	0.93	0.003	0.64		0.043		0.94	0.016	0.95
Ant	290 (±65)	0.18	0.94	0.017	0.47	0.012	0.62	0.16	0.95	0.035	0.89	0.002	0.43		0.051		0.88	0.015	0.93
			0–24 h						0–24 h						0–24 h				
Flt	8900 (±750)		0.043		0.86	0.005	0.30		0.025		0.97	«0.001	«0.01		0.006		0.50	0.005	0.98
Pyr	22 000 (±3300)		0.045		0.91	0.005	0.26		0.027		0.96	0.001	0.05		0.008		0.60	0.005	0.94
BaA	250 (±200)		0.012		0.86	0.041	0.66		0.016		0.75	0.002	0.60		0.004		0.32	0.012	0.88
Chry	130 (±23)		0.005		0.20	0.003	0.09		0.007		0.89	0.001	0.08		«0.001		«0.01	0.010	0.93
BbF	860 (±150)		0.008		0.29	−0.002	0.19		0.006		0.75	0.001	0.40		−0.001		0.06	0.001	0.59
BkF	320 (±100)		0.013		0.84	0.002	0.25		0.008		0.77	0.002	0.83		0.001		0.03	0.004	0.96
BaP	3300 (±1000)		0.016		0.92	0.001	0.10		0.012		0.77	0.002	0.62		0.003		0.23	0.003	0.89
InP	3300 (±920)		0.003		0.31	−0.001	0.02		0.001		0.32	0.002	0.71		«0.001		0.01	0.004	0.43
DaA	nd																		
BgP	8900 (±1500)		0.004		0.44	0.002	0.19		0.007		0.36	0.002	0.84		0.002		0.09	0.005	0.76

[a] 1 Standard error of the mean in parenthesis.
[b] Measured photon fluxes.
[c] Compounds are in order of molecular weight.
[d] Rate constants were calculated based on two data points.

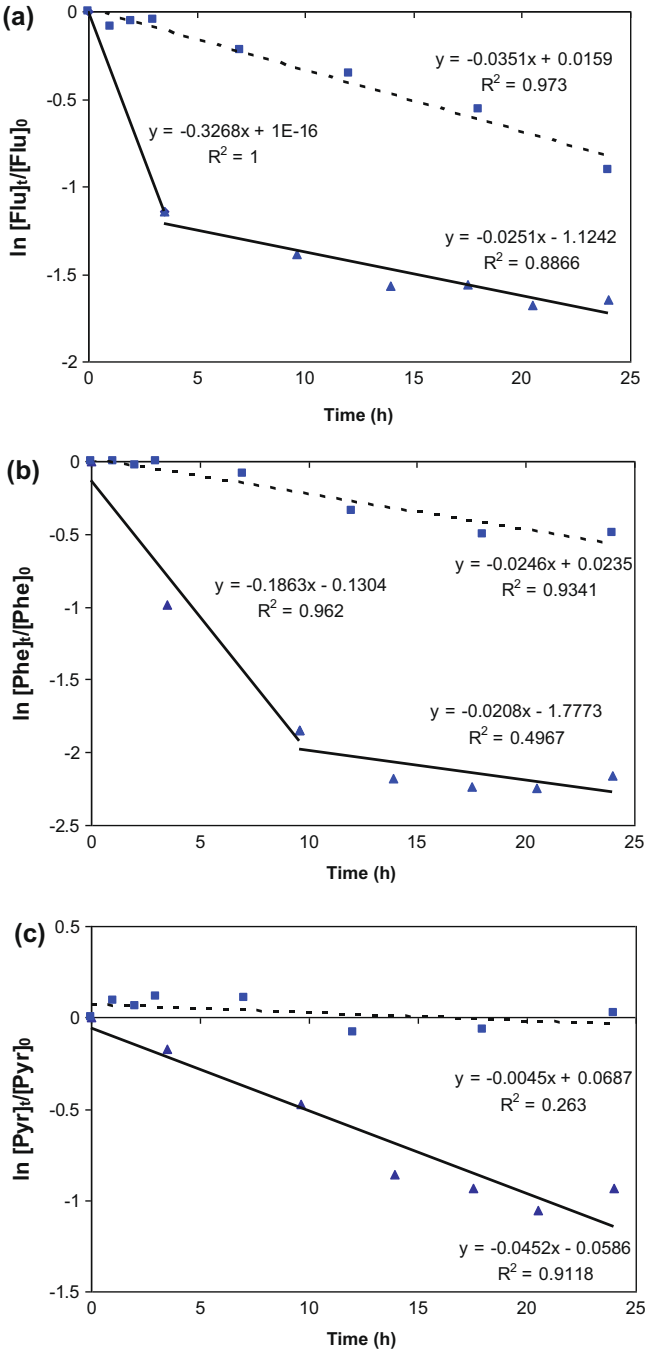

Fig. 1. First order disappearance of selected PAHs (a. fluorene, b. phenanthrene, and c. pyrene) sorbed on 2.1 mg soot particles under illumination (solid line) and in the dark at 36 °C (dashed line).

constants (0.33, 0.17 h^{-1}) for the first loss phase compared to loss rates for dark control experiments (0.035, 0.025 h^{-1}). After a significant fraction of PAHs on the surface of soot particles were lost under irradiation within 3–10 h, the disappearance of Flu and Phe became slightly slower than the loss rate under dark conditions. There was no apparent two-phase loss for Pyr but its rate constant (0.045 h^{-1}) during illumination is nine times greater than in the dark (0.005 h^{-1}). Compared to 36 °C, dark losses of PAHs associated with soot at 18 °C were dramatically lower, but remained log-linear over the entire experiment for most PAHs (Table 1). A potential mechanism consistent with the experimental findings is that the near surface lower molecular weight PAHs rapidly photodegrade and are depleted in the first phase; subsequent losses are governed by diffusion from layers closer to the soot particle centers. This diffusion rate would be slower than observed in dark controls for which near surface PAH concentrations were higher. For higher molecular weight PAHs phototransformation was slower and diffusion from deeper particle layers kept pace with photolytic loss, producing the observed "one phase" behavior.

3.3. Degradation half-lives of PAHs on soot compared to other substrates

Table 2 shows that a wide range of half-lives of particle-associated PAHs have been previously reported, at least in part because of differences in the characteristics of the substrates where PAHs were sorbed. In most cases, half-lives were calculated on the basis of rate constants for photochemical degradation without considering dark loss of PAHs. Behymer and Hites (1985) observed no concentration changes in dark control experiments; Matuzawa et al. (2001) conducted illumination of PAHs at 17 °C to reduce the effect of heat from the light source, while Wang et al. (2005) reported the total loss rate constants including photodegradation and thermal disappearance of PAHs sorbed on pine needles exposed to natural sunlight. Although Ant, BaA, and BaP are regarded as the most photoreactive components (Yunker et al., 2002), it is hard to generalize their reactivity on various substrates. In the present study, half-lives of those three PAHs in 2.1 and 4.9 mg/filter soot were very similar to each other while those on 12.7 mg of soot were 3–6 times greater. Furthermore, Ant, BaA, and BaP are not likely to photodegrade more quickly on fly ash, carbon black, or pine needles compared to other species. PAHs have common physico-chemical properties such as planar structure, hydrophobicity, low water solubility, high melting and boiling point, and low vapor pressure. Due to their conjugated structures, PAHs exhibit high light absorptivity in the UV/Vis range. The reason that high molecular weight PAHs associated with soot show relatively poor photoreactivities, however, is likely to be related to low quantum yield, possibly due to strong interactions with the substrate. Loss rate constants of PAHs were most strongly correlated with the molecular weights of PAHs rather than any other factors when the first loss phase is excluded (Fig. 2). Volatile losses would be expected to vary with molecular weight in roughly this manner, but phototransformation may also depend on molecular weight because higher molecular weight PAHs have stronger π-electron donor tendency (Zhu and Pignatello, 2005). The π–π electron donor–acceptor interactions between PAHs and soot surfaces might result in decreased phototransforma-

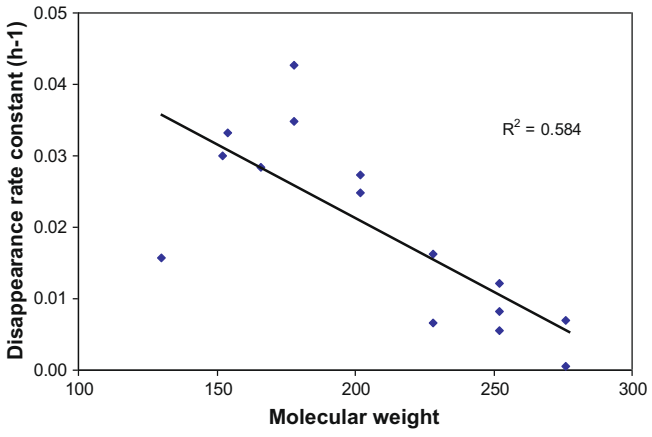

Fig. 2. Loss rate constants in the second phase as a function of the molecular weight of PAHs (4.9 mg/filter soot).

tion rates for the higher molecular weight PAHs by the decline of diffusion from inner layers to the surface because of their strong bonding.

3.4. Influence of aging on the PAH species ratios used for source apportionment

Some diagnostic PAH species ratios have been widely used for the source identification of PAHs in the environment. However, if aging alters the PAH profiles of soot particles (or other primary particulate emissions) then direct application of PAH ratios could provide the wrong information about PAH sources. This could be important in the atmosphere (where soot particles can remain suspended for approximately a week), but it is likely especially important for PAHs deposited on surfaces since the corresponding aging times can be much longer (Andreae, 2001; Kim and Young, 2009). At a given time t, the ratio of concentrations of PAHs "A" and "B" can be calculated by

$$\frac{C_t^A}{C_t^B} = \frac{C_0^A}{C_0^B} e^{(k_B - k_A)t} \quad (1)$$

$$\frac{C_t^A}{C_t^A + C_t^B} = \frac{C_0^A e^{-k_A t}}{C_0^A e^{-k_A t} + C_0^B e^{-k_B t}} = \left[1 + \frac{C_0^B}{C_0^A} e^{(k_A - k_B)t}\right]^{-1} \quad (2)$$

where C_0 is the initial concentration and k is the first-order loss rate constant at a given mass loading of soot. The second phase loss rates were used for Flt, Ant, and Phe to calculate ratios for 24–500 h. It is noted that environmental diurnal variations in temperature and actinic flux in extrapolations are needed for more accurate application of PAH ratios.

Table 3 shows the changes in some previously proposed diagnostic ratios as aging of soot-associated PAHs proceeds over extended times, resulting in changes in the source identification in some instances. Extrapolating our first-order loss rates to 500 h aging, for instance, produces an increase in the ratio of Flt/(Flt + Pyr) from 0.26–0.30 (which is in the range for a gasoline combustion source) to 0.51–0.57 (diesel combustion source), independent of the soot mass loading. Although all of our samples were from the same source, the apparent source changes with aging time based on this diagnostic ratio. Likewise, the source interpretation based on the ratio of BaA to BaA plus Chry/triphenylene (BaA/228) changed from pyrogenic to petrogenic between fresh and

Table 2
Comparison of the half-lives (h) of PAH degradation on various substrates under illumination.

	This study[a]	Pennise and Kamens[b]	Behymer and Hites[c]				Matuzawa et al.[d]			Wang et al.[e]	Niu et al.[f]
	Soot	Combusted wood chip	Silica gel	Alumina	Fly ash	Carbon black	DPM	Soil components	DPM/soil mix	Pine needles	Fly ash
Naph	44–220 (3.4–36)									10.7	
Acy	23–32(0.9–1.9)		0.7	2.2	44	170				27.7	76
Ace	21–50 (1.3–1.9)		2	2.2	44					33.0	89
Flu	21–28(1.3–3.9)		110	62	37	>1000				39.8	90
Phe	16–33 (3.6–3.7)		150	45	49	>1000	4–61	1–5	9.1	34.5	112
Ant	14–41 (3.9–4.4)		2.9	0.5	48	310				22.4	81
Flt	16–120	1–17	74	23	44	>1000	11–22	1.6–4.2	6.5	21.5	154
Pyr	15–92	0.75–7.8	21	31	46	>1000	9–734	0.8–1.6	10.2	21.9	95
BaA	5.9–180	0.8–12.4	4	2	38	650				20.6	139
Chry	110–130[g]	0.8–12.4	100	78	38	690	12–405	1.7–8.8	8.4	27.0	
BbF	84–126[g]	0.66–7								37.7	198
BkF	54–84[g]	0.66–7								28.3	248
BaP	42–280	0.11–5.7	4.7	1.4	31	570	1.6–6.6	<0.5–1.6	6.2	33.5	178
Ind	210–1200[g]	0.34–7.6								41.3	182
DaA		0.35–6								37.1	198
BgP	100–160[g]	0.31–10	7	22	29	>1000				44.1	169

[a] Values are for three different soot loadings (first phase decay half-lives in parentheses, illuminated with 1000 W xenon lamp).
[b] Exposed to natural sunlight in Pittsboro, NC.
[c] 450 W medium pressure Hg lamp used.
[d] 300 and 900 W xenon lamp used, DPM: diesel particulate matter.
[e] Exposed to natural sunlight in Dalian, China.
[f] Illuminated with simulated sunlight.
[g] Values for 12.7 mg soot were not included due to R^2 less than 0.1.

Table 3
Changes of some selected PAH source apportionment ratios (2.1/4.9/12.7 mg/filter soot) extrapolated to extended times.

	0 h	24 h	100 h	500 h	Interpretation
Ind/(Ind + BgP)	0.27/0.34/0.26	0.29/0.34/0.26	0.29/0.37/0.29	0.38/0.46/0.41	0.35–0.7 diesel emissions[a]
Flt/(Flt + Pyr)	0.29/0.26/0.30	0.31/0.27/0.31	0.33/0.32/0.34	0.53/0.57/0.51	>0.5 diesel , <0.5 gasoline[a]
BaP/(BaP + Chry)	0.98/0.97/0.94	0.97/0.97/0.93	0.98/0.95/0.92	0.13/0.69/0.81	0.49 diesel, 0.73 gasoline[a]
BaP/BgP	0.44/0.38/0.45	0.33/0.33/0.44	0.13/0.23/0.42	«0.01/0.03/0.30	>0.6 traffic emission[a]
Ind/BgP	0.37/0.52/0.34	0.38/0.52/0.36	0.41/0.59/0.40	0.62/0.85/0.70	~0.4 gasoline, ~1 diesel[a]
Ant/178	0.18/0.16/0.16	0.21/0.23/0.14	0.28/0.43/0.06	0.65/0.94/«0.01	>0.1 combustion, <0.1 petroleum[b]
BaA/228[d]	0.66/0.68/0.77	0.12/0.60/0.73	«0.01/0.41/0.69	«0.01 / 0.01/0.31	<0.2 petroleum, >0.35 combustion[b]
Phe/Ant	4.48/5.40/5.34	3.82/3.44/6.07	2.59/1.35/15.1	0.54/0.06/291	<10 pyrogenic, >15 petrogenic[c]
Flt/Pyr	0.41/0.34/0.43	0.44/0.37/0.45	0.50/0.46/0.52	1.15/1.30/1.02	~1 pyrogenic, «1 petrogenic[c]

[a] Ravindra et al. (2006) and therein.
[b] Budzinski et al. (1997).
[c] Baumard et al. (1998).
[d] Triphenylene was not monitored in this study and BaA/228 was calculated based on data from BaA and Chry.

aged soot samples of 2.1 and 4.9 mg/filter. For our 2.1 and 4.9 mg/filter soot samples and aging conditions, the Ant to Ant plus Phe (Ant/178) and Phe/Ant ratios provided the correct diagnosis that the samples were combustion-derived at all times. However, Ant/178 and Phe/Ant ratios in the 12.7 mg/filter soot sample are changed enormously after 100 and 500 h of aging, suggesting that the loss mechanism of Phe and Ant sorbed on a large amount of soot particles under illumination would be significantly different from other cases. The ratio BaA/228 correctly indicated pyrogenic origin initially but indicated petrogenic origin after 500 h of aging. Other ratios designed to differentiate between gasoline and diesel provided ambiguous results in all cases. If fast photodegradation of PAHs are added for the calculation of PAH ratios over extended time, then the difference between predicted values based on PAH profile and real ones will be further enhanced. When the aging effect and various mass loadings of soot were considered, therefore, there was no ratio that could be universally used for PAH source identification. Many researchers, of course, have developed other useful methods for the prediction of PAH sources that are not considered in Table 3. In addition, particulate PAHs deposited on land can also degrade through biological and other abiotic processes not considered here.

4. Conclusions

This work demonstrates the loss rates for PAHs associated with soot particles under illumination and the validity of some diagnostic PAH ratios for source apportionment of aged PAHs. An apparent two-phase disappearance in all experiments was observed for Naph, Acy, Ace, and Flu, while Phe and Ant exhibited this behavior for all but the highest soot loading. Only a single mode of disappearance, however, was observed for the higher molecular weight PAHs with 4–6 rings. The observed results might be related to molecular sizes, intrinsic photolysis rates, and interaction between PAHs and soot particles. Further investigation is needed to determine contributions of the direct photolysis and the diffusion kinetics to the apparent disappearance rates of PAHs on soot. Due to differences in disappearance rates of individual PAHs, prolonged exposure to sunlight could change the interpretation of some diagnostic ratios used widely for PAH source identification. Unlike PAHs in aerosol which are relatively fresh, therefore, sources of PAHs from surface waters and sediments should be determined by considering the potential influence of aging on any diagnostic method.

Acknowledgments

The project described was supported by Grant No. P42ES004699 from the National Institute of Environmental Health Sciences. The content is solely the responsibility of the authors and does not necessarily represent the official views of the National Institute of Environmental Health Sciences or the National Institutes of Health.

References

Anastasio, C., McGregor, K.G., 2001. Chemistry of fog waters in California's Central Valley: 1. In situ photoformation of hydroxyl radical and singlet molecular oxygen. Atmos. Environ. 35, 1079–1089.

Andreae, M.O., 2001. The dark side of aerosol. Nature 409, 671–672.

Baumard, P., Budzinski, H., Michon, Q., Garrigues, P., Burgeot, T., Bellocq, J., 1998. Origin and bioavailability of PAHs in the Mediterranean See from mussel and sediment records. Estuar. Coast. Shelf S. 47, 77–90.

Behymer, T.D., Hites, R.A., 1985. Photolysis of polycyclic aromatic hydrocarbons adsorbed on simulated atmospheric particulates. Environ. Sci. Technol. 19, 1004–1006.

Behymer, T.D., Hites, R.A., 1988. Photolysis of polycyclic aromatic hydrocarbons on fly ash. Environ. Sci. Technol. 22, 1311–1319.

Berner, B.A., Wise, S.A., Currie, L.A., Klouda, G.A., Klinedinst, D.B., Zweidinger, R.B., Stevens, R.K., Lewis, C.W., 1995. Distinguishing the contributions of residential wood combustion and mobile source emissions using relative concentrations of dimethylphenanthrene isomers. Environ. Sci. Technol. 29, 2383–2389.

Boehm, P.D., Farrington, J.W., 1984. Aspects of the polycyclic aromatic hydrocarbon geochemistry of recent sediments in the Georges Bank region. Environ. Sci. Technol. 18, 840–845.

Dickhut, R.M., Canuel, E.A., Gustafson, K.E., Liu, K., Arzayus, K.M., Walker, S.E., Edgecombe, G., Gaylor, M.O., Mcdonald, E.H., 2000. Automotive sources of carcinogenic polycyclic aromatic hydrocarbons associated with particulate matter in the Chesapeake Bay region. Environ. Sci. Technol. 34, 4635–4640.

Douben, P.E.T. (Ed.), 2003. PAHs: An Ecotoxicological Perspective. John Wiley & Sons, Chichester, UK.

Dreyer, A., Radke, M., Turunen, J., Blodau, C., 2005. Long-term change of polycyclic aromatic hydrocarbon deposition to peatlands of Eastern Canada. Environ. Sci. Technol. 39, 3918–3924.

Eganhouse, R.P. (Ed.), 1997. Molecular Markers in Environmental Geochemistry. American Chemical Society, Washington, DC.

Hannigan, M.P., Cass, G.R., Penman, B.W., Crespi, C.L., Lafleur, A.L., Busdy, W.F.J., Thilly, W.G., Simoneit, B.R.T., 1998. Bioassay-directed chemical analysis of Los Angeles airborne particulate matter using human cell mutagenicity assay. Environ. Sci. Technol. 32, 3502–3514.

Hwang, H.-M., Foster, G.D., 2006. Characterization of polycyclic aromatic hydrocarbons in urban stormwater runoff flowing into the tidal Anacostia River, Washington, DC, USA. Environ. Pollut. 140, 416–426.

Jacob, J., 1996. The significance of polycyclic aromatic hydrocarbons as environmental carcinogens. Pure Appl. Chem. 68, 301–308.

Kamens, R.M., Guo, Z., Fulcher, J.N., Bell, D.A., 1988. Influence of humidity, sunlight, and temperature on the daytime decay of polyaromatic hydrocarbons on atmospheric soot particles. Environ. Sci. Technol. 22, 103–108.

Kim, D., Young, T.M., 2009. Significance of indirect deposition on wintertime PAH concentrations in an urban Northern California creek. Environ. Eng. Sci. 26, 269–278.

Korfmacher, W.A., Wehry, E.L., Mamantov, G., Natusch, D.F.S., 1980. Resistance to photochemical decomposition of polycyclic aromatic hydrocarbons vapor-adsorbed on coal fly ash. Environ. Sci. Technol. 14, 1094–1099.

Lee, J.H., Gigliotti, C.L., Offenberg, J.H., Eisenreich, S.J., Turpin, B.J., 2004. Sources of polycyclic aromatic hydrocarbons to the Hudson River Airshed. Atmos. Environ. 38, 5971–5981.

Matuzawa, S., Nasser-Ali, L., Garrigues, P., 2001. Photolytic behavior of polycyclic aromatic hydrocarbons in diesel particulate matter deposited on the ground. Environ. Sci. Technol. 35, 3139–3143.

NIOSH (1999). Elemental Carbon (Diesel Particulate): Method 5040 (<http://origin.cdc.gov/niosh/nmam/pdfs/5040f3.pdf>).

Niu, J., Sun, P., Schramm, K.-W., 2007. Photolysis of polycyclic aromatic hydrocarbons associated with fly ash particles under simulated sunlight irradiation. J. Photochem. Photobiol. A. 186, 93–98.

Orecchio, S., 2007. PAHs associated with the leaves of Quercus ilex L: extraction, GC–MS analysis, distribution and sources: assessment of air quality in the Palermo (Italy) area. Atmos. Environ. 41, 8669–8680.

Oros, D.R., Ross, J.R.M., 2005. Polycyclic aromatic hydrocarbons in bivalves from the San Francisco estuary: spatial distributions, temporal trends, and sources (1993–2001). Mar. Environ. Res. 60, 466–488.

Pennise, D.M., Kamens, R.M., 1996. Atmospheric behavior of polychlorinated dibenzo-p-dioxins and dibenzofurans and the effect of combustion temperature. Environ. Sci. Technol. 30, 2832–2842.

Prahl, F.G., Carpenter, R., 1983. Polycyclic aromatic hydrocarbon (PAH)-phase associations in Washington coastal sediment. Geochim. Cosmochim. Acta 47, 1013–1023.

Ravindra, K., Bencs, L., Wauters, E., De Hoog, J., Deutsch, F., Roekens, E., Bleux, N., Berghmans, P., Grieken, R.V., 2006. Seasonal and site-specific variation in vapour and aerosol phase PAHs over Flanders (Belgium) and their relation with anthropogenic activities. Atmos. Environ. 40, 771–785.

Readman, J.W., Mantoura, R.F., Rhead, M.M., 1984. The physico-chemical speciation of polycyclic aromatic hydrocarbons (PAH) in aquatic systems. Fresen. Z. Anal. Chem. 319, 126–131.

Schauer, J.J., Rogge, W.F., Hildemann, L.M., Mazurek, M.A., Cass, G.R., Simoneit, B.R., 1996. Source apportionment of airborne particulate matter using organic compounds as tracers. Atmos. Environ. 30, 3837–3855.

Schmidt, M.W., Noack, A.G., 2000. Black carbon in soils and sediments: analysis, distribution, implications and current challenges. Global Biogeochem. Cy. 14, 777–793.

Sicre, M.A., Marty, J.C., Saliot, A., Aparicio, X., Grimalt, J., Albaiges, J., 1987. Aliphatic and aromatic hydrocarbons in different sized aerosols over the Mediterranean Sea: occurrence and origin. Atmos. Environ. 21, 2247–2259.

Wang, D., Chen, J., Xu, Z., Qiao, X., Huang, L., 2005. Disappearance of polycyclic aromatic hydrocarbons sorbed on surfaces of pine [Pinua thunbergii] needles under irradiation of sunlight: volatilization and photolysis. Atmos. Environ. 39, 4583–4591.

Yu, S., Jones, A.D., Chang, D.P.Y., Kelly, P.B., Kennedy, I.M., 1998. The transformation of chromium in a laminar premixed hydrogen-air flame. P. Combust. Inst. 27, 1639–1645.

Yunker, M.B., Macdonald, R.W., Vingarzan, R., Mitchell, R.H., Goyette, D., Sylvestre, S., 2002. PAHs in the Fraser River basin: a critical appraisal of PAH ratios as indicators of PAH source and composition. Org. Geochem. 33, 489–515.

Zhang, X.L., Tao, S., Liu, W.X., Yang, Y., Zuo, Q., Liu, S.Z., 2005. Source diagnostics of polycyclic aromatic hydrocarbons based on specific ratios: a multimedia approach. Environ. Sci. Technol. 39, 9109–9114.

Zhu, D., Pignatello, J.J., 2005. Characterization of aromatic compounds sorptive interactions with black carbon (charcoal) assisted by graphite as a model. Environ. Sci. Technol. 39, 2033–2041.